data

MDPI

Data Descriptor

A Consistent Land Cover Map Time Series at 2 m Spatial Resolution—The LifeWatch 2006-2015-2018-2019 Dataset for Wallonia

Julien Radoux [1,*], Axel Bourdouxhe [2], Thomas Coppée [2], Mathilde De Vroey [1], Marc Dufrêne [2] and Pierre Defourny [1]

[1] Earth and Life Institute, Université Catholique de Louvain, B-1348 Louvain-la-Neuve, Belgium
[2] Gembloux AgroBioTech, Université de Liège, B-4000 Liège, Belgium
* Correspondence: julien.radoux@uclouvain.be

Abstract: Ecosystem accounting is based on the definition of the extent and the status of an ecosystem. Land cover maps extents are representative of several ecosystems and can therefore be used to support ecosystem accounting if reliable change information is available. The dataset described in this paper aims to provide land cover information (13 classes) for biodiversity monitoring, which has driven two key features. On one hand, open areas were described in more details (5 classes) than in the other maps available in the study area in order to increase their relevance for biodiversity models. On the other hand, monitoring means that the time series must consist of comparable layers. The time series integrate information from existing high quality land cover maps that are not fully comparable, as well as thematic products (crop type, road network and forest type) and remote sensing data (25 cm orthophotos, 0.8 pts/m^2 LIDAR and Sentinel-1&2 data). Because of the high spatial resolution of the data and the fragmented landscape, boundary errors could cause a large proportion of false change detection if the maps are classified independently. Buildings and forests were therefore consolidated across time in order to build a time series where these changes can be trusted. Based on an independent validation, the overall accuracy was 93.1%, 92.6%, 94.8% and 93.9% +/−1.3% for the years 2006, 2015, 2018 and 2019, respectively. The specific assessment of forest patch change highlighted a 98% +/−2.7% user accuracy across the 4 years and 85% of forest cut detection. This time series will be completed and further consolidated with other dates using the same protocol and legend.

Dataset: The dataset (vx18) can be visualized and downloaded from the following web portal https://maps.elie.ucl.ac.be/lifewatch.

Dataset License: CC-BY

Keywords: land cover; map; landscape; remote sensing; biodiversity

Citation: Radoux, J.; Bourdouxhe, A.; Coppée, T.; De Vroey, M.; Dufrêne, M.; Defourny, P. A Consistent Land Cover Map Time Series at 2 m Spatial Resolution—The LifeWatch 2006-2015-2018-2019 Dataset for Wallonia. *Data* **2023**, *8*, 13. https://doi.org/10.3390/data8010013

Academic Editors: Juan-Carlos Jiménez-Muñoz and Juanle Wang

Received: 31 October 2022
Revised: 14 December 2022
Accepted: 24 December 2022
Published: 31 December 2022

1. Summary

This paper describes four 2 m raster land cover maps, which were designed for the characterization of the Lifewatch ecotope database [1]. The dataset was produced in the frame of the Belgian contribution to Lifewatch-ERIC, the European Research Infrastructure Consortium for biodiversity and ecosystem research. This set of maps, version vx18, resulted from remote sensing image analysis (orthophotos and Sentinel-1&2) consolidated and enriched by ancillary data in order to provide relevant land cover information for biodiversity models. It distinguishes four classes of open landscapes often grouped in a single "grassland" category in other land cover maps: intensively managed grasslands, dry open areas of biological interest, inundated herbaceous cover and post-disturbance herbaceous vegetation. The temporal consistency of the data was a major concern of the processing chain, and therefore also of the validation framework, because change

information is an important component of the temporal analysis. The quality of the map was assessed with state-of-the-art sampling design, response design and analysis. It achieved a maximum overall accuracy of 94.8 in 2018, and 98% user accuracy of forest change across the different epochs. The consolidation process will continue when new dates are added.

2. Data Description

2.1. Data Format

The data are a set of four single band raster images at 2 m resolution. The total area mapped is 16,902 km^2. It is stored in compressed cloud optimized GeoTIFF format with georeferencing information (Belgian Lambert 2008 projection, EPSG:3812). Pyramids with modal resampling and color tables were added using the GDAL library so that it can be easily opened and visualized in any Geographic Information System or Image Analysis Software. The land cover classes are stored in byte (unsigned 8 bits integers) to minimize the size of the data on disk. These classes are further described in Section 2.2, and the data are illustrated in Figure 1 for the year 2018, showing its full extent, and in Figure 2, which is a spatial subset with the four different dates.

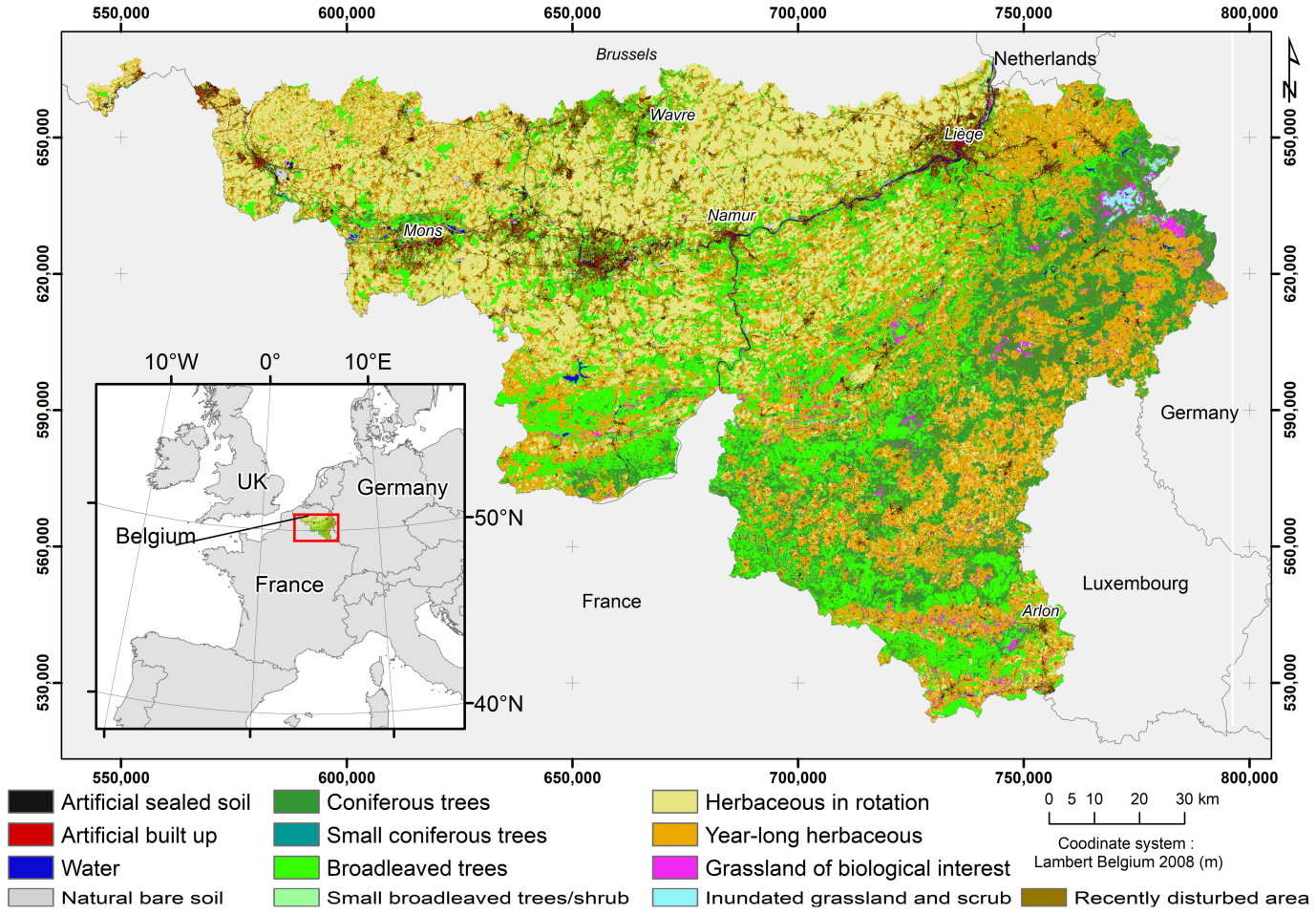

Figure 1. Wallonia's land cover map 2018 displayed with its 13 classes.

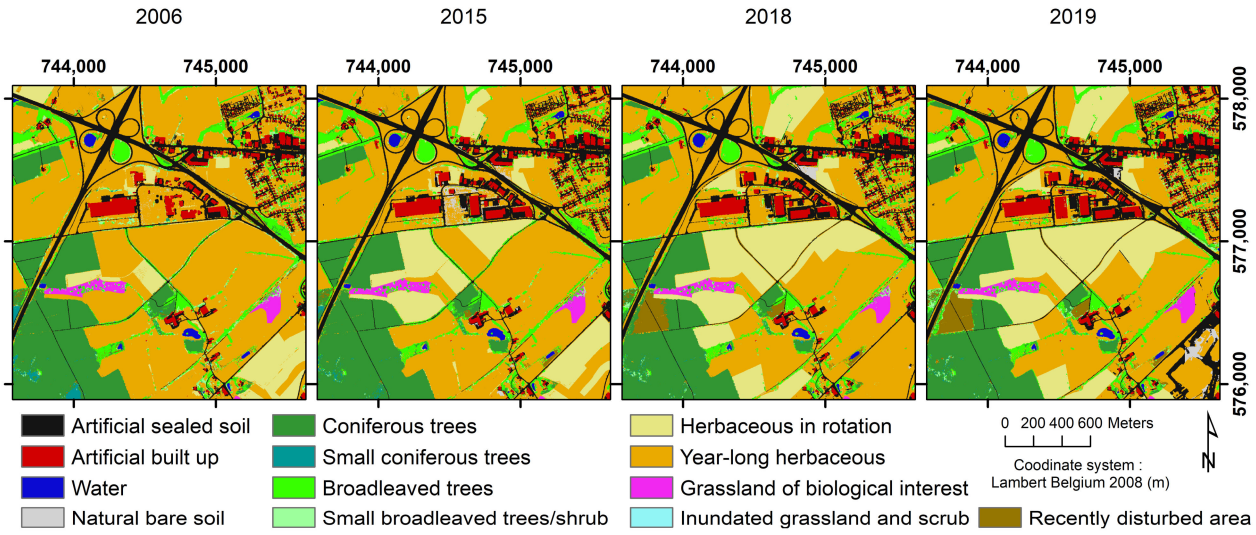

Figure 2. Subset of the time series illustrating different types of land cover change.

2.2. Land Cover Legend

Land cover is defined as the physical and biological cover of the land surface, including artificial surfaces, agricultural areas, forests, (semi-)natural areas, wetlands and water bodies. The legend of this data series includes 13 classes. Table 1 provides the numeric code of each class as well as the percentage that it covered over Wallonia in 2018.

Table 1. Land cover classes of the Lifewatch land cover map and their percentage of land area based on the 2018 classification. The total mapped area is 16,902 km^2.

Map Class	Map Code	Related EAGLE Code	Percentage of Land Area [%] Based on 2018 Product
Water	10	LCC-3	0.73
Natural Material Surfaces with less than 10% vegetation	15	LCC-1_2	0.32
Artificially sealed ground surface	20	LCC-1_1_1_3	5.75
Building, specific structures and facilities	21	LCC-1_1_1_1 | | LCC-1_1_1_2	1.99
Herbaceous in rotation during the year (e.g., crops)	30	LCC-2_2	23.94
Grassland with intensive management	35	LCC-2_2	27.57
Grassland and scrub of biological interest	40	LCC-2_2	1.82
Inundated grassland and scrub of biological interest	45	LCC-2_2 & LCH-4_4_2	0.22
Vegetation of recently disturbed area (e.g., clear cut)	48	LCC-2_2 & LCH-3_8	2.64
Coniferous trees (≥3 m)	50	LCC-2_1_1 & LCH-3_1_1	11.24
Small coniferous trees (<3 m)	51	LCC-2_1_2 & LCH-3_1_1	0.40
Broadleaved trees (≥3 m)	55	LCC-2_1_1 & LCH-3_1_2	21.63
Small broadleaved trees (<3 m) and shrubs	56	LCC-2_1_2 & LCH-3_1_2	1.75

Classes are described at their upper level according to a strict land cover point of view. The definition of the classes is compatible with the guidelines of the European Environment Information and Observation Network (EIONET), which is a partnership network of the European Environment Agency (EEA) and its 38 member and cooperating countries. More precisely, the legend matches the EAGLE (EIONET Action Group on Land monitoring in Europe) guidelines [2] for land cover component mapping (EAGLE matrix

3.1.2). The EAGLE concept is a framework for the integration of land cover and land use information from various data sets in one single data model. However, the definition of the classes of the Lifewatch land cover legend has been adapted at a finer level in order to account for management practices that have a strong impact on the biodiversity potential of otherwise similar vegetation types. The choices were also guided by the feasibility of the implementation of the classification, the compatibility with other legends and their importance for biodiversity models. Finally, the label structure differs in order to stress the similarities in terms of land cover and functional traits:

- Natural Material Surfaces (LCC-1_2) and water (LCC-3): This group includes open water bodies and rivers as well as natural material surfaces such as rocks in cliffs or geological layers exposed by extraction activities. Those surfaces should not be covered with more than 10% of vegetation.
- Artificial Surfaces and Constructions (LCC-1_1): This group includes artificially sealed soils such as roads, parking areas or compacted soils in industrial areas, as well as all types of man-made above-ground buildings. The two subtypes are separated based on their height above the ground, except for bridges that are set on the ground.
- Woody vegetation (LCC-2_1): This group includes trees and shrubs, either needle-leaved (coniferous) or broad-leaved (angiosperm). They are first separated based on the leaf type because it is more discernable than structure. It is worth nothing that most of the coniferous trees in the region are sempervirens, while most of the broadleaved trees are deciduous. However, there are some rare exceptions in both cases, such as larches (Larix sp.) for the deciduous coniferous and box-tree (Buxus sempervirens) for the sempervirens broadleaved. Each tree type class is further subdivided based on the height observed by photogrammetry. The small trees (less than 3 m) include hedgerows, young forest regrowth and small tree or shrub plantations, such as Christmas trees (coniferous), vineyard (broadleaved) or low-stemmed orchards (broadleaved).
- Herbaceous vegetation (LCC-2_2): This class regroups all vegetation cover dominated by non-ligneous species, i.e., forbs or graminoids in the study area. They are primarily distinguished based on the temporality of the vegetation (presence or absence of bare soil during the year), which in fact reflects the management practice (ploughing of crop fields) or recent land cover disturbance, such as clear cut. When the vegetation cover remains during the whole season, a further distinction is performed to highlight biodiversity difference. Dry and inundated herbaceous covers of high biodiversity are separated from more intensively managed grasslands, such as intensive pastures, high productive meadows, sport fields, urban park, private gardens, etc.

2.3. Strengths of the LC Map Series

Apart from its high overall accuracy, the main strength of this land cover time series is the consistency of the land cover classification through time in order to preserve boundaries on the majority of unchanged pixels. Figure 2 illustrates several land cover changes, including forest clear cut, new buildings, switch from year-long grassland to ploughed agricultural parcel and bare soil on a construction site. On the other hand, other boundaries remain unchanged, and forest types are consistent despite the different phenological stages in the input orthophotos. This consistency is a methodological choice to avoid false change detections due to class similarities or geometric differences along edges. The classification is indeed driven by change detection before and after the classification so that overestimating land cover change proportions is strongly reduced with regards to a simple comparison of independent maps. The second strength of this map is its thematic precision in an open area. While this precision does not replace the thematic details from field-based biological maps, preliminary studies with the dataset showed that accounting for these classes can boost the performance of biodiversity models [3,4].

2.4. Accuracy Assessment

For the validation, good practices in point-based map validation were followed according to the state of the art [5]. We used a probabilistic sampling design, fully independent of the classification process. The primary validation, used to build the confusion matrix, was based on photo-interpretation of the 2015 orthophotos (25 cm resolution) complemented in 2016 with field verification when there was a doubt about the photo-interpreted class. In total, 1200 points were visually classified. The uncertain points (121) were verified on the field, out of which 64 points were correct. Fifteen of the unsure points could not be verified in the field due to accessibility constraints. Those were double-checked by a second operator and existing ancillary data, which confirmed the first photointerpretation. Because of the risk to underestimate the classification accuracy due to positional errors, the spatially closest class in a 5 m radius was also provided by the operator. If a pixel label does not match the primary label but does with the secondary label, it is verified on the map that the incorrect primary labelling is only due to the spatial mismatching of the boundary between the two classes on the map or on the orthophoto. In this case, the secondary label replaces the primary label in the reference. The same points were verified on the orthophotos of 2006/2007, 2015 and 2018 and 2019.

The samples were selected in a double-stratified probabilistic sampling design in order to get clusters of points and hence potentially reduce the displacements for the field-based verification stage. The first stratification level was based on five biogeographical regions of Wallonia. The second stratification level was 5 km by 5 km grid cells. When a grid cell was located across several biogeographical regions, its labels were defined based on the location of its centroid. Ten cells were randomly selected for each region. At the second stage, a total of 25 points was randomly selected inside each grid cell. Points lying out of Walloon region were discarded so that a total of 1200 samples made the validation dataset.

Due to the stratification based on biogeographical areas (Figure 3), the sampling rate was not uniform. The proportion of correctly classified pixels was therefore computed for each region. Those values were then aggregated for Wallonia with weight that is inversely proportional to the sampling probability (in other words, directly proportional to the area of the discretized biogeographical region). The uncompletedness due to the cell-based coverage of Wallonia is neglected because the matching between the regular grid and the true extent is more than 99%: this sample is therefore considered fully representative of the sampled area.

In addition, another sample was taken to check the user accuracy of forest patch (areas of continuous tree cover of minimum 1000 m^2) change detection. This additional sample consisted of 100 points randomly selected inside forest patches, where at least one forest change occurred between 2006 and 2019 based on the time series.

3. Validation Results

Photointerpretation results were adjusted to take into account errors due to slight misregistration (one pixel) and residual parallax errors. Furthermore, small gaps or roads under the trees are not visible on the orthophotos and therefore do not appear in the validation dataset. This was managed by trusting LIDAR data for the detection of small forest gaps (in addition to the orthophotos) and ancillary vector data for the road network.

Because of the stratified sampling, a weight (w) is assigned to each point depending on the stratum (i) to which the point belongs. The weight is proportional to the area of the class (S_i) divided by the total area of the map, and inversely proportional to the number of points taken in each class (n) [5].

The estimated overall accuracy (OA) with a geometric tolerance of one pixel reaches 93.1%, 92.6%, 94.8% and 93.9% +/−1.3%, respectively, for 2006, 2015, 2018 and 2019. This is statistically larger than the targeted 90% with a confidence level of 95%. Table 2 shows the confusion matrix for the year 2018 along with the user's and producer's accuracies. The user's accuracy (UA) is defined as the probability, for each class, that the label of a pixel is correct; the producer's accuracy (PA) is the probability that a field feature is correctly classified on

the map. The mean map UA is 92% and the mean map PA, 86%. The confusion matrices, including geometric errors, are provided in the Appendix A for 2006, 2015, 2018 and 2019 respectively. These geometric errors reduce approximately 4% of the overall accuracy.

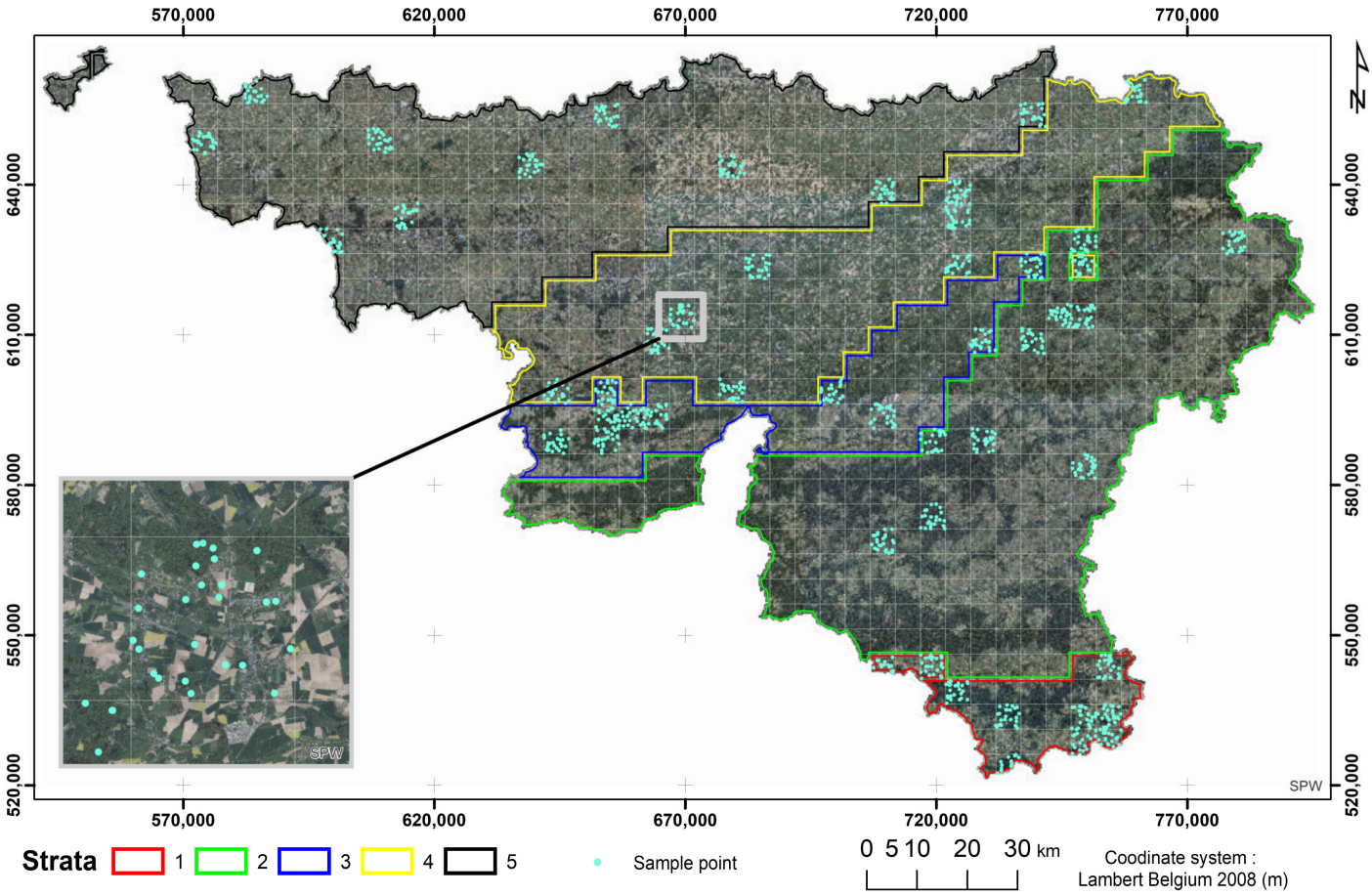

Figure 3. Distribution of the sample points selected by stratified probabilistic sampling. The first stratification is based on bio-geographical regions of Wallonia. Sets of 25 points are then selected inside randomly selected grid cells (white lines). The orthophoto of 2018 is used as background (Service Public de Wallonie, 2018).

Nine out of thirteen classes have very good (>85%) class-based accuracy values, but bare soils, dry herbaceous cover with high biodiversity potential and small trees are less good. This is due to a combination of technical and conceptual reasons. On one hand, many orthoimages were taken in a leafless period for the trees/shrubs, and therefore, deciduous vegetation was hardly visible. Second, because of the size of the elements, Sentinel-2 spatial resolution was insufficient to add the complementary information in these cases [6]. On the other hand, some of these classes are part of an ecological gradient with fuzzy limits between classes (e.g., between intensively and extensively managed grasslands) defined by arbitrary thresholds (height threshold for shrubs, time threshold to consider that a recently disturbed area becomes an open area of biological interest).

About 13% of the validation samples occurred in areas of observed change. The user accuracy of the change detection was 82%, 61% and 73% for 2006–2015, 2015–2018 and 2018–2019, respectively. Most of the false change detection is due to geometric discrepancies. For statistical analysis of areal land cover change, the rounded confusion matrices of the 4 years—not corrected for geometric errors—are provided in the Appendix A for 2006, 2015, 2018 and 2019 respectively, and the precise confusion matrices are provided as Supplementary Materials.

Table 2. Confusion matrix accounting for the stratification for the year 2018. UA stands for user's accuracy and PA for producer's accuracy. The colors correspond to the legend of the maps. Values are rounded. See Table 1 for the complete class and color descriptions.

Ref \ Cl	10	15		21	30	35	40	45	48	50	51	55	56	PA
10	14.8													100
15		3.0	1.5											67
			64.3			0.2							0.5	99
21				24										100
30					238		0.5							99.8
35			1.5	1.5	1.5	282	0.5		2.1			3.2	1.5	95.9
40	1.5					5.1	17.5		0.7	0.7				68.7
45								1.7						100
48			0.2			1.7			31.9	2.1		2.3	1.7	80
50			1.9							164		3.8	0.2	96.5
51						1.7			1.7	2.1	3.2		3.3	26.4
55			2.7						1.5	10.5		280	3.3	93.9
56									1.1				14.4	93.2
UA	90.7	100	89.1	100	99.4	97.0	95.1	100	82.0	91.4	100	96.8	57.8	

More specifically, forest change detection proved to have a large user accuracy (98/100) based on the additional point sample of forest change pixels. The two errors were due to the false detection of "non forest" to "forest" while all the "forest" to "non forest" changes were correct. Considering the large user and producer accuracy of the forest class as a whole (95.8 and 96.8), forest ecosystem monitoring with this dataset can be seen as highly reliable. The points used to build the confusion matrix were screened to estimate the producer accuracy of the forest change detection. Amongst the 569 points that were forest at some stage, 85% of the tree loss were correctly detected. It is worth noting that 7 out of 8 omissions consisted in clear cuts between the year 2006 and 2015, while the remaining one was a thinning between 2018 and 2019.

4. Methods

Because of the good quality of other land-cover-related data in the Walloon region (91.5% for Walous 2018 [7] and 90.7% for WalousMàJ 2019 [8]), the overall approach of this research focused on the consistency of the land cover mapping through time. The upgrade of the initial classification (done in the year 2015) therefore applied to all unchanged pixels of each year.

4.1. Input Data

The main imagery source is a set of 2.5 Tb mosaic of orthorectified aerial images acquired in 2006/2007, 2015 and 2018 at 25 cm of resolution. The images are collected from the end of winter to the end of summer, with a majority of the acquisitions occurring in early spring. There are therefore large differences in terms of vegetation phenology between and within the years of the three mosaics.

Using photogrammetry, a digital surface model (DSM) is built from each orthophoto. By subtracting the digital surface model (DSM) based on a 1 m resolution DEM from LIDAR data of 2013, it is then possible to derive a digital height model (DHM). The DHM is unfortunately not usable for vegetation height when the photographs are captured during the leafless period, but it is otherwise a reliable source to detect major land cover changes.

In addition to the airborne datasets, time series from the Sentinel-1 and -2 satellites provide information about temporal dynamic LC features (grassland in rotation, difference between broadleaved and coniferous trees). Sentinel-1 10 m resolution images are acquired every 2 to 6 days by C-Band SAR instrument, while the Sentinel-2 instrument records multispectral reflectance at 10 and 20 m resolution every 3 (on overlapping scenes) or 5 days (in non-overlapping areas). These images were not available in 2006.

Walous 2018 and WalousMàJ 2019 and additional thematic information was used for specific land cover classes. A forest type map was used to consolidate the discrimination of broadleaved and coniferous trees. The anonymized Land Parcel Identification System, a parcel level database including crop type information declared by farmers in the framework of the Common Agricultural Policy of the European Union, was used for the agricultural areas. Finally, the NATURA 2000 database was used to identify some of the areas of high biodiversity interest.

4.2. Data Processing

Most of the image processing used the Orfeo Toolbox library [9]. Image classification was performed as a combination of random forest and deep learning with locally trained models. The deep learning was a U-Net model focusing on buildings, for which geometry plays a major role in the identification. The grassland of potential high biodiversity was screened based on late mowing detection with Sentinel-1 and Sentinel-2 satellites, as described in [10], as well as a specific multiyear random forest classification of the orthophotos. The anonymized LPIS data were used to discriminate crop fields as temporary grassland ploughed during the year based on the class of the previous year. The different datasets were resampled at 2 m resolution because it was a good compromise between classification accuracy and geometric precision.

For the temporal consistency, pixel-based change detection with iterative trimming was used to identify areas of potential change [11] and focus the classification only on these areas. Forest types and open area types were forced based on the majority rule for all years when change was unlikely. Furthermore, in order not to contaminate change detection with geometric errors, a single stable boundary was selected for each feature with a vertical dimension. It is indeed well-known that uncomplete orthorectification overestimates the area of tall objects due to the parallax effect when they are viewed from an oblique angle by the airborne camera. Therefore, a set of morphological mathematics tools was used to clean the boundaries of buildings and trees.

For buildings and roads, Walous 2018 was selected as a geometric reference because it was consolidated with official vector datasets [7]. Buildings or roads that exist in 2018 and at another date are identified using the intersection of 2-pixel dilation of their extent. If the intersection with 2018 is not void, the geometry of 2018 is used. Otherwise, newly detected geometries are used.

For trees, the same leaf type is forced for all dates if the series of labels is not interrupted by a clear-cut detection. The forcing is selected with a majority voting of the different classified orthophotos, Sentinel-2 classification and forest type map of Wallonia. The minimum extent of small woody elements (hedges, tree alignments, and isolated trees) is used, and the outside pixels are removed within a buffer. A temporal closing is also applied on these woody elements to fill gaps in the time series in case a pixel not classified as tree on date "t" was classified in "t − 1" and "t + 1".

Large areas (>1000 m^2) of inconsistencies between the different classifier were visually checked and manually corrected when the photointerpretation was certain. This consolidation phase was necessary to reach the very high overall accuracy of this map, especially in open areas or with thin forest patches not clearly discriminable with Sentinel-2.

5. User Notes

The data described in this paper comprise a biodiversity-oriented land cover map series with a spatial resolution of 2 m. It is provided as a GeoTIFF file supported in any GIS software. Its legend is enriched with subclasses of shrubs and grasslands. Even if the discrimination amongst those classes remains less accurate than for the other classes, they provide a strong added value for ecosystem and habitat mapping.

Improving the temporal consistency of the LC series is a major challenge at 2 m resolution because of the prevalence of geometric errors from year to year. In order to reduce false change detection in fragmented areas, where the relative impact of geometric

discrepancies is maximal, a conservative approach was used for the representation of small woody features. As a result, it is worth noting that the smallest woody features are likely to be underestimated. This is not highlighted in the quantitative results due to the small area covered by these land cover features. On the other hand, despite the consolidation, some classification errors still contaminate the change detection of some classes. It is therefore important to take the confusion matrices (provided in the Supplementary Material as Tables S1–S4 into account for further diachronic analysis based on the time series.

Gradients naturally occur between various classes. At the spatial resolution of the dataset, mixed pixels are proportionally less problematic than at a coarse resolution. However, there is no strict boundary between the intensive grasslands. In this case, there is a gradient that is a combination of different land use intensities (fertilization level, mowing frequency, and pasture intensity). Most of the grasslands in the study area belong to one of the two extremes: they are either strongly artificialized (intensively managed agricultural lands, and residential grasslands) or natural grassland. Some private gardens could be of great interest for biodiversity, but this could not be captured in this map because of their small size on average.

Land cover only reflects one component of the landscape. Users interested in more thematic details are therefore invited to cross this dataset with the land use and biotope information, which already exist on the territory. This information and the proportions described in this paper are integrated in the Lifewatch ecotopes database [1].

Supplementary Materials: The following supporting information can be downloaded at: https://www.mdpi.com/article/10.3390/data8010013/s1. Table S1: unrounded values of the confusion matrix for the year 2006, Table S2: unrounded values of the confusion matrix for the year 2015, Table S3: unrounded values of the confusion matrix for the year 2018 and Table S4: unrounded values of the confusion matrix for the year 2019.

Author Contributions: Conceptualization, J.R., M.D. and P.D.; Formal analysis, J.R.; Methodology, J.R., M.D.V., T.C., A.B., M.D. and P.D.; Project administration, J.R., M.D. and P.D.; Resources, J.R., T.C., M.D.V. and M.D.; Software, J.R.; Supervision, M.D. and P.D.; Validation, T.C. and J.R.; Visualization, J.R.; Writing—original draft, J.R.; Writing—review and editing, All. All authors have read and agreed to the published version of the manuscript.

Funding: This research was funded by the Fédération Wallonie-Bruxelles in the frame of the contribution of Belgium to Lifewatch-ERIC, the European Research Infrastructure Consortium for biodiversity and ecosystem research.

Institutional Review Board Statement: Not applicable.

Informed Consent Statement: Not applicable.

Data Availability Statement: The dataset (vx18) can be visualized and downloaded from the following web portal https://maps.elie.ucl.ac.be/lifewatch (accessed on 25 November 2022).

Acknowledgments: Computational resources have been partially provided by the supercomputing facilities of the Université catholique de Louvain (CISM/UCLouvain) and the Consortium des Équipements de Calcul Intensif en Fédération Wallonie Bruxelles (CÉCI) funded by the Fond de la Recherche Scientifique de Belgique (F.R.S.-FNRS) under convention 2.5020.11 and by the Walloon Region.

Conflicts of Interest: The authors declare no conflict of interest. The funders had no role in the design of the study; in the analyses or interpretation of data; in the writing of the manuscript. They agreed on the decision to publish the results.

Appendix A

Table A1. Confusion matrix for the year 2006. The overall accuracy is 89.4%. Color and class descriptions are available in Table 1. Unrounded values are provided as Supplementary Material.

Ref \ Cl	10	15		21	30	35	40	45	48	50	51	55	56	PA
10	13.3		0.5											89.8
15		1.7				1.5								50
			53.9	2.1		2.8						3.6	0.5	85.7
21			1.5	21.5										93.4
30					224	0.7	0.5							98.8
35		1.1	4.5	2.6	4.1	275			2.6			5.9	3.6	91.9
40			2.2			7.6	12.8		1.3	1.7		1.5	0.9	45.8
45								1.7						100
48					1.7				8.4	0.4	1	0.6	3.2	54.5
50			1.9						4	166	1.7	3.4	1.1	93.3
51										0.5	21.4		1.7	91
55	1.5		6.2		1.5	6.1			3.6	15.8	3.6	241	9.3	83.5
56						1.1					1.1		32.9	94
UA	89.8	58.9	76.8	82.1	96.9	92.8	96.6	100	42.2	90.0	74.5	93.6	61.9	

Appendix B

Table A2. Confusion matrix for the year 2015. The overall accuracy is 88.6%. Color and class descriptions are available in Table 1. Unrounded values are provided as Supplementary Material.

Ref \ Cl	10	15		21	30	35	40	45	48	50	51	55	56	PA
10	14.4		0.5											97.0
15		1.7	1.5											53.3
			57	1.1	2.3							3.6	0.5	88.4
21			1.5	22.5										93.7
30					242		0.5							99.8
35			7.1	2.6	3.0	260	0.5		3.8	1.7	1	6.4	2.6	90.1
40	1.5	0.5	1.7		1.5	6.7	10.9		0.7	2.3			0.5	41.5
45								1.7						100
48			0.2			1.7			39.9			2.3	1.7	87.2
50			1.9						2.9	154		3.8	0.2	94.6
51						1.7			1.7	2.6	2.1		3.3	18.5
55	1.5		5.5			3.3			3.2	16.4	0.2	265	3.3	94
56						0.5							14	96.9
UA	82.6	79.3	74.1	86.2	98.2	94.2	92.3	100	76.5	87.0	62.3	94.3	54	

Appendix C

Table A3. Confusion matrix for the year 2018. The overall accuracy is 90.7%. Color and class descriptions are available in Table 1. Unrounded values are provided as Supplementary Material.

Ref \ Cl	10	15		21	30	35	40	45	48	50	51	55	56	PA
10	14.8													100
15		3.0	1.5											66.7
			57.0	1.1		2.8						3.6	0.5	87.8
21			1.5	22.5										93.7
30					238		0.5							99.8
35			3.5	2.6	3.0	268	0.5		2.1			8.9	2.6	92.0
40	1.5		2.2			5.6	11.1		0.7	4			0.5	43.5
45								1.7						100
48			0.2			1.7			30.3	3.8		2.3	1.7	75.8
50			1.9						2.9	161		3.8	0.2	94.8
51						1.7			1.7	2.1	3.1		3.3	26.4
55	1.5		5.5			3.3			1.1	16.4	0.2	264	3.3	88.7
56									1.5				14.0	90.7
UA	83.0	100	77.8	86.2	98.7	94.7	92.5	100	71.4	85.9	93.7	93.4	53.7	

Appendix D

Table A4. Confusion matrix for the year 2019. The overall accuracy is 89.4%. Color and class descriptions are available in Table 1. Unrounded values are provided as Supplementary Material.

Ref \ Cl	10	15		21	30	35	40	45	48	50	51	55	56	PA
10	13.3					1.5								89.8
15		3.0												100
			53.9	2.1		2.8						3.6	0.5	85.7
21			1.5	21.5										93.4
30					236	1.7	0.5					1.5		98.5
35		2.6	5.4	2.6	4.7	263			2.1	1.5		10.4	1.1	89.6
40			2.2			7.1	12.8		2.2	2.1		1.5	0.5	45.1
45								1.7						100
48						1.7			19.1	7.3		2.5	3.2	56.4
50			1.9						2.9	168	1.7	5.5		93.3
51						1.7			1.7	2.6	2.1		3.3	21.9
55	1.5		5.7			3.6			5.1	17.5	0.2	259	3.3	87.5
56									1			1.7	11	79.9
UA	89.8	54.1	76.3	82.1	98.1	92.9	96.6	100	55.8	84.4	53.0	90.6	52.1	

References

1. Radoux, J.; Bourdouxhe, A.; Coos, W.; Dufrêne, M.; Defourny, P. Improving ecotope segmentation by combining topographic and spectral data. *Remote Sens.* **2019**, *11*, 354. [CrossRef]
2. Available online: https://land.copernicus.eu/eagle/work-results-documentation-and-tools (accessed on 25 November 2022).
3. Delangre, J.; Radoux, J.; Dufrêne, M. Landscape delineation strategy and size of mapping units impact the performance of habitat suitability models. *Ecol. Inform.* **2018**, *47*, 55–60. [CrossRef]
4. Bourdouxhe, A.; Duflot, R.; Radoux, J.; Dufrêne, M. Comparison of methods to model species habitat networks for decision-making in nature conservation: The case of the wildcat in southern Belgium. *J. Nat. Conserv.* **2020**, *58*, 125901. [CrossRef]
5. Olofsson, P.; Foody, G.; Herold, M.; Stehman, S.; Woodcock, C.; Wulder, M. Good Practices for Assessing Accuracy and Estimating Area of Land Change. *Remote Sens. Environ.* **2013**, *148*, 42–57. [CrossRef]
6. Radoux, J.; Chomé, G.; Jacques, D.C.; Waldner, F.; Bellemans, N.; Matton, N.; Lamarche, C.; d'Andrimont, R.; Defourny, P. Sentinel-2's potential for sub-pixel landscape feature detection. *Remote Sens.* **2016**, *8*, 488. [CrossRef]
7. Bassine, C.; Radoux, J.; Beaumont, B.; Grippa, T.; Lennert, M.; Champagne, C.; De Vroey, M.; Martinet, A.; Bouchez, O.; Deffense, N.; et al. First 1-M Resolution Land Cover Map Labeling the Overlap in the 3rd Dimension: The 2018 Map for Wallonia. *Data* **2020**, *5*, 117. [CrossRef]
8. Draime, D.; Denies, J.; Stephenne, N. 2022 Updating the Walloon land cover map by operational application of artificial intelligence with a deep local authorities' appropriation. In Proceedings of the ESA Living Planet Symposium, Bonn, Germany, 23–27 May 2022; Available online: https://express.converia.de/frontend/index.php# (accessed on 25 November 2022).
9. Grizonnet, M.; Michel, J.; Poughon, V.; Inglada, J.; Savinaud, M.; Cresson, R. Orfeo ToolBox: Open source processing of remote sensing images. *Open Geospat. Data Softw. Stand.* **2017**, *2*, 1–8. [CrossRef]
10. De Vroey, M.; de Vendictis, L.; Zavagli, M.; Bontemps, S.; Heymans, D.; Radoux, J.; Kotez, B.; Defourny, P. Mowing detection using Sentinel-1 and Sentinel-2 time series for large scale grassland monitoring. *Remote Sens. Environ.* **2022**, *280*, 113145. [CrossRef]
11. Radoux, J.; Lamarche, C.; Van Bogaert, E.; Bontemps, S.; Brockmann, C.; Defourny, P. Automated training sample extraction for global land cover mapping. *Remote Sens.* **2014**, *6*, 3965–3987. [CrossRef]